Investigation of the Properties of Galactic Cosmic Rays with the KASCADE-Grande Experiment

J.R. Hörandel [a,j], W.D. Apel [b], J.C. Arteaga [a,k], F. Badea [b], K. Bekk [b], M. Bertaina [c], J. Blümer [b,a], H. Bozdog [b], I.M. Brancus [d], M. Brüggemann [e], P. Buchholz [e], E. Cantoni [c,f], A. Chiavassa [c], F. Cossavella [a], K. Daumiller [b], V. de Souza [a,ℓ], F. Di Pierro [c], P. Doll [b], R. Engel [b], J. Engler [b], M. Finger [b], D. Fuhrmann [g], P.L. Ghia [f], H.J. Gils [b], R. Glasstetter [g], C. Grupen [e], A. Haungs [b], D. Heck [b], T. Huege [b], P.G. Isar [b], K.-H. Kampert [g], D. Kang [a], D. Kickelbick [e], H.O. Klages [b], P. Łuczak [h], H.J. Mathes [b], H.J. Mayer [b], B. Mitrica [d], C. Morello [f], G. Navarra [c], S. Nehls [b], J. Oehlschläger [b], S. Ostapchenko [b], S. Over [e], M. Petcu [d], T. Pierog [b], H. Rebel [b], M. Roth [b], H. Schieler [b], F. Schröder [b], O. Sima [i], M. Stümpert [a], G. Toma [d], G.C. Trinchero [f], H. Ulrich [b], A. Weindl [b], J. Wochele [b], M. Wommer [b], J. Zabierowski [h]

[a] *Institut für Experimentelle Kernphysik, Universität Karlsruhe, Germany*
[b] *Institut für Kernphysik, Forschungszentrum Karlsruhe, Germany*
[c] *Dipartimento di Fisica Generale dell'Università di Torino, Italy*
[d] *National Institute of Physics and Nuclear Engineering, Bucharest, Romania*
[e] *Fachbereich Physik, Universität Siegen, Germany*
[f] *Istituto di Fisica dello Spazio Interplan etario, INAF Torino, Italy*
[g] *Fachbereich Physik, Universität Wuppertal, Germany*
[h] *Soltan Institute for Nuclear Studies, Lodz, Poland*
[i] *Department of Physics, University of Bucharest, Bucharest, Romania*
[j] *now at: Radboud University Nijmegen, Department of Astrophysics, P.O. Box 9010, 6500 GL Nijmegen, The Netherlands*
[k] *now at: Universidad Michoacana, Morelia, Mexico*
[ℓ] *now at: Universidade de São Paulo, Instituto de Física de São Carlos, Brasil*

Abstract

The properties of galactic cosmic rays are investigated with the KASCADE-Grande experiment in the energy range between 10^{14} and 10^{18} eV. Recent results are discussed. They concern mainly the all-particle energy spectrum and the elemental composition of cosmic rays.

Key words: cosmic rays, energy spectra, mass composition, extensive air showers
PACS: 96.50.S-, 96.50.sb, 96.50.sd, 98.70.Sa

1. Introduction

To reveal the origin of galactic cosmic rays is the main objective of the KASCADE and KASCADE-Grande experiments. The results of KASCADE contributed significantly to the understanding of the origin of the knee in the all-particle energy spectrum of cosmic rays at energies around $4 \cdot 10^{15}$ eV. It could be shown that the knee is caused by a fall-off in the flux of light nuclei [1,2]. Energy spectra for five dominant elemental groups could be reconstructed (p, He, CNO, Si, and Fe), they exhibit a fall-off behavior approximately proportional to the nuclear charge of the elemental groups. In the energy region between 10^{17} and 10^{18} eV a transition from a galactic to an extra-galactic origin of cosmic rays is expected [3]. Main focus of KASCADE-Grande is to understand the end of the galactic cosmic-ray component through detailed investigations of the energy spectrum and the mass composition in this energy region.

KASCADE-Grande comprises 37 detector stations equipped with plastic scintillators, covering an area of 0.5 km^2 to measure the electromagnetic shower component [4]. It also includes the original KASCADE experiment,

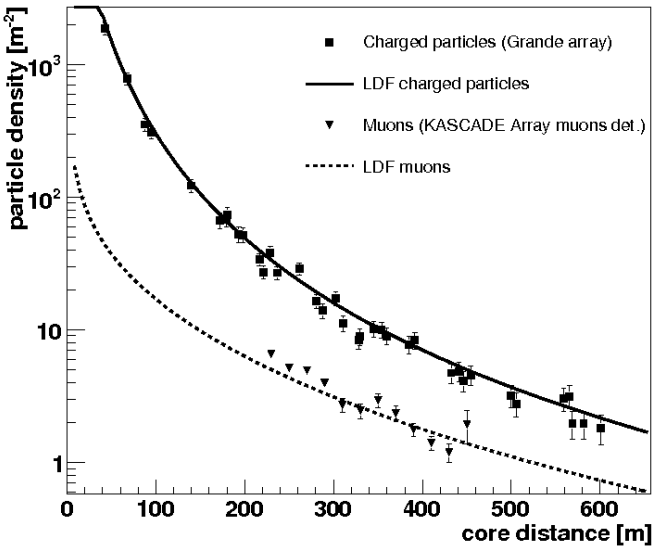

Fig. 1. Measured lateral distribution of a single event for charged particles and muons [9].

consisting of several detector systems [5]. A 200×200 m^2 array of 252 detector stations, equipped with scintillation counters, measures the electromagnetic and, below a lead/iron shielding, the muonic parts of air showers. A 130 m^2 streamer tube detector, shielded by a soil-iron absorber serves to reconstruct the tracks of high-energy ($E_\mu > 0.8$ GeV) muons [6]. An iron sampling calorimeter of 16×20 m^2 area detects hadronic particles [7]. It has been calibrated with a test beam at the SPS at CERN up to 350 GeV particle energy [8].

As an example for a measured air shower, the lateral distributions for charged particles and for muons are shown in Fig. 1 [9]. The charged-particle density is measured with the Grande detectors and the muonic component by the shielded array detectors of KASCADE.

2. Test of hadronic interaction models

The astrophysical interpretation of air shower data requires detailed knowledge of the properties of hadronic interactions at energies and kinematical ranges beyond the capabilities of present-day accelerator experiments. Therefore, air shower data are used to constrain hadronic interaction models used in air shower simulations, such as the CORSIKA [10] code. Several hadronic interaction models have been systematically tested over the last decade.

First quantitative tests [11,12,13] established QGSJET 98 [14] as the most compatible code. Similar conclusions have been drawn for the successor code QGSJET 01 [15]. Recently, a new method has been developed to measure the attenuation of hadrons in air showers [16]. This method is very sensitive to inelastic hadronic cross sections. The investigations indicate, that the inelastic cross sections in QGSJET 01 are slightly too large ($\approx 5\%$ at 10^6 GeV). Predictions of QGSJET II [17,18,19] exhibit problems when compared to air shower data [20], in particular, the predicted electron-hadron correlations are not compatible with the measurements.

Predictions of SIBYLL 1.6 [21] were not compatible with air shower data, in particular there were strong inconsistencies for hadron-muon correlations. These findings stimulated the development of SIBYLL 2.1 [22]. This model proved to be very successful, the predictions of this code are fully compatible with KASCADE air shower data [23,24,15].

Investigations of the VENUS [25] model revealed some inconsistencies in hadron-electron correlations [13]. The predictions of neXus 2 [26] were found to be incompatible with the KASCADE data, in particular, when hadron-electron correlations have been investigated [15]. Recently, predictions of the interaction model EPOS 1.61 [27,28,29] have been compared to KASCADE air shower data [30]. The analysis indicates that EPOS 1.61 delivers not enough hadronic energy to the observation level and the energy per hadron seems to be too small. These findings stimulated the development of a new version EPOS 1.9 [31]. Corresponding investigations with this new version are under way and results are expected to be published soon.

Analyses of the predictions of the DPMJET model yield significant problems in particular for hadron-muon correlations for the version DPMJET 2.5 [32], while the newer version DPMJET 2.55 is found to be compatible with air shower data [15].

Presently, the most compatible predictions are obtained from the models QGSJET 01 and SIBYLL 2.1.

3. Muons in air showers

The lateral distribution of muons ($E_\mu > 230$ MeV) is investigated using the shielded detectors of the original KASCADE array up to distances to the shower axis exceeding 600 m [33]. A function suggested by Lagutin and Raikin is used to described the measured muon densities as a function of the distance to the shower axis. This method allows to reconstruct the total number of muons in air showers with an accuracy better than 20%.

A comparison of measured muon densities to predictions of air shower simulations indicates that these observable is sensitive to differences in hadronic interaction models [34]. The muon density has been measured as a function of the total number of electrons in the showers, i.e. as a function of primary energy.

Muons with energies exceeding 800 MeV are investigated with the muon tracking detector. Lateral distributions have been measured, they can be described by a Lagutin-like function [36]. The information of the reconstructed muon tracks is used to obtain radial and tangential angles with respect to the shower axis. These quantities, in turn, are applied to infer the pseudorapidity distributions of secondary particles in hadronic interactions which decay into muons [37].

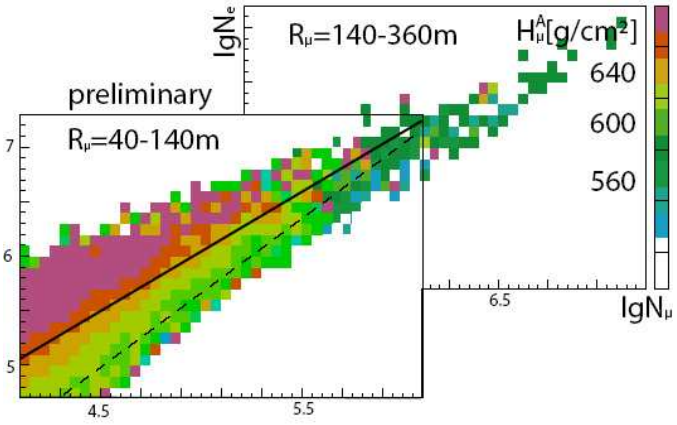

Fig. 2. Effective depth of the muon production H_μ^A in the $N_e - N_\mu$ plane for showers with zenith angle smaller than 18° [35]. Diagrams are overlayed for separate KASCADE and KASCADE-Grande analyses.

The muon tracks are also used to measure the production height of muons in the atmosphere by means of triangulation [35]. The corresponding production depth of muons in the atmosphere is depicted in Fig. 2 in the $N_e - N_\mu$ plane. The figure combines two separate analyses for the energy ranges of KASCADE and KASCADE-Grande, respectively. In the electron-muon number plane light particles are expected to be to the upper left of the main diagonal. In this region large muon production depths are reconstructed. This indicates light particles, penetrating deep into the atmosphere. The measured air showers are classified in four intervals of the muon production depth. For these intervals the primary energy spectrum is reconstructed, based on the measured number of electrons and muons. This yields energy spectra for four elemental groups. The spectra exhibit a fall-off for the light component at low energies (several 10^{15} eV), while the all-particle spectrum at high energies is dominated by heavy nuclei [35].

4. All-particle energy spectrum

Different methods are applied to the data to reconstruct the all-particle energy spectrum.

The density of charged particles at large distances from the shower axis is a good mass-independent estimator for the shower energy [38]. The particular optimum radial distance depends on the layout and altitude of the detector array, for KASCADE-Grande a distance of 500 m yields best values and we use the charged-particle density $S(500)$ at 500 m from the shower axis as energy estimator. The constant intensity cut method is applied to evaluate the attenuation behavior of the $S(500)$ values. Thus, the all-particle energy spectrum is reconstructed.

Another analysis takes advantage of the total number of charged particles measured for each air shower [39]. The shower size spectra measured in different zenith angle intervals are used to obtain the attenuation length for this observable. The constant intensity cut method is again applied to correct for attenuation effects and the primary energy spectrum is obtained.

In a similar way the muon data have been analyzed [40]. The constant intensity cut method is used to correct for the attenuation of the measured total number of muons in different zenith angle intervals. Again, predictions of air shower simulations are used to establish an energy scale for the observed quantities and the all-particle energy spectrum is derived from the observed number of muons.

The last analysis discussed here, combines information from charged particles and muons [41]. Independent fits to the lateral distributions of charged particles and muons allow to extract the number of charged particles and number of muons for each shower. These quantities are used to assign an energy to each shower on an event-by-event basis. Thus, the all-particle energy spectrum is inferred.

The results obtained with the different methods are compiled in Fig. 3. The reconstructed all-particle flux is shown as a function of the primary energy. The arrow indicates a typical systematic uncertainty of the energy scale of the order of 20%. Since the elemental composition is presently not clear in this energy region, for some methods two spectra are plotted, one for proton induced showers and a second one for iron induced showers. The different methods agree well for a heavy dominated mass composition around energies of 10^{17} eV [43]. The spectra obtained in the energy range between 10^{16} and 10^{18} eV smoothly extend the energy spectrum as measured by KASCADE to high energies. The new results match as well the flux obtained by other experiments, shown in the figure as well.

5. Composition

First analyses have started to reveal the elemental composition at the end of the galactic component [44]. They use the measured number of electrons and muons and indicate that these observables are indeed sensitive to the elemental composition. At present, the measured data can be described by a fit of three elemental groups. A comparison of the measured electron-to-muon number ratio from KASCADE-Grande to similar data obtained with KASCADE yields consistent results.

Ultimate goal is a deconvolution of the measured size spectra for the electromagnetic/charged and the muonic shower components, similar to the unfolding procedure applied to KASCADE data [1] to obtain energy spectra for separate elemental groups at energies up to 10^{18} eV.

6. Conclusions and outlook

The recent results from the KASCADE-Grande experiment indicate that we make substantial progress in measuring the energy spectrum and the elemental composition of cosmic rays in the energy region between 10^{16} and 10^{18} eV. The new data will significantly contribute to the

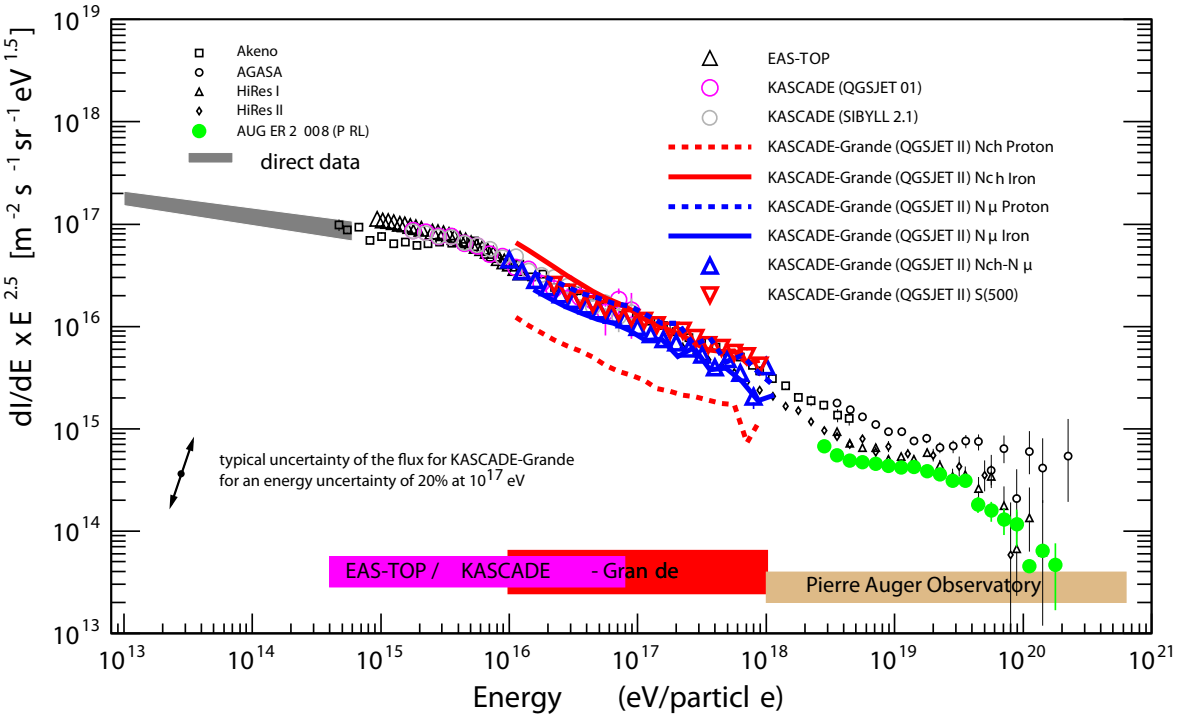

Fig. 3. All-particle energy spectrum of cosmic rays. Spectra obtained with different methods applied to KASCADE-Grande data are compared to results of other experiments [42].

understanding of the end of the galactic component and the transition to an extra-galactic component. The data will be crucial to distinguish between different astrophysical scenarios.

References

[1] T. Antoni, et al., Astropart. Phys. 24 (2005) 1.
[2] W. D. Apel, et al., Astropart. Phys. 31 (2009) 86–91.
[3] J. Blümer, R. Engel, J. Hörandel, Prog. Part. Nucl. Phys. (2009) in press (arXiv 0904.0725).
[4] G. Navarra, et al., Nucl. Instr. & Meth. A 518 (2004) 207.
[5] T. Antoni, et al., Nucl. Instr. & Meth. A 513 (2003) 490.
[6] P. Doll, et al., Nucl. Instr. & Meth. A 488 (2002) 517.
[7] J. Engler, et al., Nucl. Instr. & Meth. A 427 (1999) 528.
[8] S. Plewnia, et al., Nucl. Instr. & Meth. A 566 (2006) 422.
[9] F. Di Pierro, et al., Proc. 31th Int. Cosmic Ray Conf., Lodz (2009) # 895.
[10] D. Heck, et al., Report FZKA 6019, Forschungszentrum Karlsruhe (1998).
[11] J. R. Hörandel, et al., Nucl. Phys. Proc. Suppl. 75A (1999) 228–233.
[12] J. Hörandel, Proc. 26th Int. Cosmic Ray Conf., Salt Lake City 1 (1999) 131.
[13] T. Antoni, et al., J. Phys. G: Nucl. Part. Phys. 25 (1999) 2161.
[14] N. Kalmykov, et al., Nucl. Phys. B (Proc. Suppl.) 52B (1997) 17.
[15] W. Apel, et al., J. Phys. G: Nucl. Part. Phys. 34 (2007) 2581.
[16] W. Apel, et al., Phys. Rev. D 80 (2009) 022002.
[17] S. Ostapchenko, astro-ph/0412591 (2005).
[18] S. Ostapchenko, Phys. Rev. D 74 (2006) 014026.
[19] S. Ostapchenko, Nucl. Phys. B (Proc. Suppl.) 151 (2006) 143 and 147.
[20] J. Hörandel, et al., Proc. 31th Int. Cosmic Ray Conf., Lodz (2009) # 227.
[21] J. Engel, et al., Phys. Rev. D 46 (1992) 5013.
[22] R. Engel, et al., Proc. 26th Int. Cosmic Ray Conf., Salt Lake City 1 (1999) 415.
[23] J. Milke, et al., Acta Physica Polonica B 35 (2004) 341.
[24] J. Milke, et al., Proc. 29th Int. Cosmic Ray Conf., Pune 6 (2005) 125.
[25] K. Werner, Phys. Rep. 232 (1993) 87.
[26] H. Drescher, et al., Phys. Rep. 350 (2001) 93.
[27] K. Werner, F. Liu, T. Pierog, Phys. Rev. C 74 (2006) 044902.
[28] T. Pierog, et al., Proc. 30th Int. Cosmic Ray Conf., Merida 4 (2008) 629.
[29] T. Pierog, K. Werner, arXiv:astro-ph 0611311 (2006).
[30] W. Apel, et al., J. Phys. G: Nucl. Part. Phys. 36 (2009) 035201.
[31] T. Pierog, et al., Proc. 31th Int. Cosmic Ray Conf., Lodz (2009) # 428.
[32] J. Ranft, Phys. Rev. D 51 (1995) 64.
[33] D. Fuhrmann, et al., Proc. 31th Int. Cosmic Ray Conf., Lodz (2009) # 131.
[34] V. de Souza, et al., Proc. 31th Int. Cosmic Ray Conf., Lodz (2009) # 499.
[35] P. Doll, et al., Proc. 31th Int. Cosmic Ray Conf., Lodz (2009) # 429.
[36] P. Łuczak, et al., Proc. 31th Int. Cosmic Ray Conf., Lodz (2009) # 220.
[37] J. Zabierowski, et al., Proc. 31th Int. Cosmic Ray Conf., Lodz (2009) # 171.
[38] G. Toma, et al., Proc. 31th Int. Cosmic Ray Conf., Lodz (2009) # 347.
[39] D. Kang, et al., Proc. 31th Int. Cosmic Ray Conf., Lodz (2009) # 1044.
[40] J. Arteaga-Velázquez, et al., Proc. 31th Int. Cosmic Ray Conf., Lodz (2009) # 805.
[41] M. Bertaina, et al., Proc. 31th Int. Cosmic Ray Conf., Lodz (# 323).
[42] W. Apel, et al., arXiv 0906.4007 (2009).

[43] A. Haungs, et al., Proc. 31th Int. Cosmic Ray Conf., Lodz (# 401).
[44] E. Cantoni, et al., Proc. 31th Int. Cosmic Ray Conf., Lodz (2009) # 524.